

Integrated Optical Modulator for Adaptive Digital Modulation and Analogue Applications

Atsushi Kanno, Isao Morohashi, Takahide Sakamoto, Tetsuya Kawanishi
National Institute of Information and Communications Technology
4-2-1 Nukui-kitamachi, Koganei, Tokyo 184-8795, Japan
Email: kanno@nict.go.jp

Abstract—Adaptive digital modulation in the optical domain is performed using an integrated optical modulator with a high symbol rate of 10 Gbaud. The optical digital-to-analogue conversion technique that employs an optical IQ modulator and a dual-polarization quadrature-phase-shift-keying (DP-QPSK) modulator is applicable to binary PSK, QPSK, and 16-ary quadrature amplitude modulation. Analogue modulation such as radio-over-fiber signal generation is also demonstrated using the integrated modulators, with high phase stability.

I. INTRODUCTION

There is a great demand for high-speed connections between ground stations (GND) and communication satellites on a geo-stationary earth orbit (GEO) for the transfer of high-resolution images for surveillance of the earth; there is also a need for a ubiquitous broadband connection for situations in which an optical fiber cannot be deployed. In disaster recovery situations, in particular, high-speed satellite communication plays an important role because other broadband communications such as optical fiber and high-speed mobile communications, whose base stations are generally connected to the optical fiber, are disrupted at a disaster [1]. In fact, a wideband inter-networking engineering test and demonstration satellite (WINDS), called “Kizuna,” helped in realizing a broadband connection between the anti-disaster headquarters and the local disaster measure offices during the Great East Japan earthquake of March 11th, 2011 [2]. Because survival rate is significantly decreased within 72 h of a disaster, quick deployment of the broadband communication link helps keep damage to a minimum. Moreover, key facilities such as nuclear power plants always require a broadband protection link for information to be surveyed remotely. The realization of reliable connectivity has been one of the most important issues involved in maintaining a data rate. A loss in connection has significant implications for surveillance satellites such as the Mars Pathfinder and Voyager.

An adaptive modulation technique is a possible candidate as a solution to these issues owing to its feature of high reliable connectivity. The reason for this is that a suitable modulation scheme can be adaptively changed, depending on various signal-to-noise ratios (SNRs) at the receiver. However, a radio-communication-based electrical method using an IQ modulator limits the transmission speed because of the bandwidth of these electrical components, such as a digital-to-analogue converter (DAC), and as a result, the data rates could be as high as

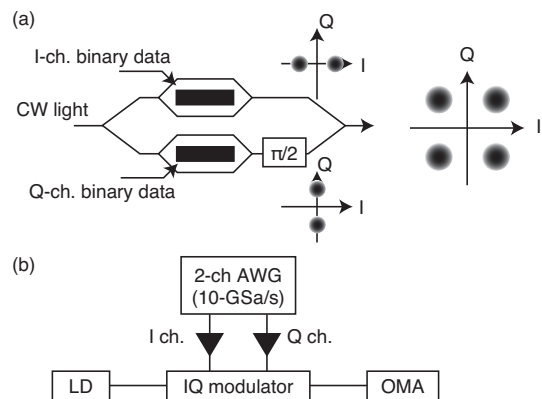


Fig. 1. (a) Schematic illustration of an optical IQ modulator for QPSK modulation, and (b) experimental setup.

several Gb/s. Optical space communication technology could increase this capacity to possibly even exceed 10 Gb/s [3], [4]. Moreover, a coherent communication technique would help increase the data rate as well as the sensitivity, so that this technique would be one of the most important features of next-generation high-speed space communication between the GND-GEO and inter-satellite links, such as the GEO to low earth orbit (LEO) satellites [5]–[7]. In this scenario, an optical modulation technique for high-speed coherent communication would be greatly needed. Recently, an integrated lithium niobate (LN) modulator for optical fiber communication was developed rapidly with the development of a digitally aided optical coherent detection technique. A 100 gigabit ethernet (100GbE) requires dual-polarization quadrature-phase-shift-keying (DP-QPSK) modulation for optimization of the spectral efficiency, and 28-Gbaud operation with this modulator realizes a line rate of 112 Gb/s and a data rate of 100 Gb/s [8]. For installing a line card at a rack of routers, the reduction of the footprint forces an integrated modulator to be developed monolithically. Nowadays, the development of high-frequency electrical circuit design, accurate optical waveguide design, and the associated fabrication technologies have helped realize 64-ary quadrature amplitude modulation (QAM) optical signal generation in a single integrated modulator as well as high-symbol-rate optical modulation greater than 80 Gbaud [9]–[12].

In this paper, we discuss an adaptive modulation technique

based on an integrated optical modulator developed for optical fiber communication. An increase in the number of nested Mach-Zehnder interferometer (MZI) modulators can optimize the resolution of an optical DAC. High-speed adaptive modulation with 10-Gbaud operation using an integrated optical LN modulator is demonstrated with a binary PSK (BPSK), QPSK, and 16-QAM, which have a spectral efficiency of 1, 2, and 4 b/s/Hz, respectively, resulting in line rates of 10, 20, and 40 Gb/s, respectively. The integrated modulator of the DP-QPSK modulator, which is a type of a quad-parallel MZI modulator, can easily generate a radio-over-fiber (RoF) signal with high stability for the demonstration of high-speed radio signal generation as an analogue application [13].

II. ADAPTIVE DIGITAL MODULATION USING OPTICAL DAC

To realize an assured connection, the optimization of the SNR plays an important role. The reason for this is that the SNR depends on the emitted laser power as well as on the modulation format. Thus, an adaptive modulation technique becomes indispensable for a reliable connection.

A. IQ Modulator

An IQ modulator is one of the most well-known and common modulator structures not only in optical communication, but in radio communication as well. A schematic of an optical IQ modulator is shown in Fig. 1(a). An IQ modulator generally comprises of two nested MZI modulators, which work as a phase and intensity modulator, in a main MZI for optimization of the phase relationship between the two arms. The relative optical phase can be optimized by controlling the bias voltage of the main MZI. Because the relative phase is set at $\pi/2$, the nested MZIs can provide optical signals as in-phase and quadrature phase components.

In general, an advanced modulation format such as multi-level modulation or orthogonal-frequency-domain-multiplexing can only be realized in an IQ modulator with a technique that is similar to a modern radio communication technique. However, high-symbol-rate modulation greater than 20 Gbaud is still difficult because of the issue of the linearity of the modulator drivers as well as the issue of a low-speed electrical DAC and its resolution. The operation voltage of an LN optical modulator, the so-called half-wave voltage $V\pi$, is more than about 3 V, and thus, the modulator drivers are indispensable for operation. Moreover, for the realization of higher-order multi-level modulation, a high resolution with high-speed operation is required for the electrical DAC function.

An optical DAC using parallel nested MZI modulators would be one of the possible candidates for high-symbol-rate multi-level modulation without the need for electrical DACs and linear modulator drivers. When each nested MZI launched by an electrical binary signal is operated under a full swing condition at a null bias point (which is only for BPSK, for example), a transfer function of the optical modulator with a sinusoidal response provides clear symbol separation

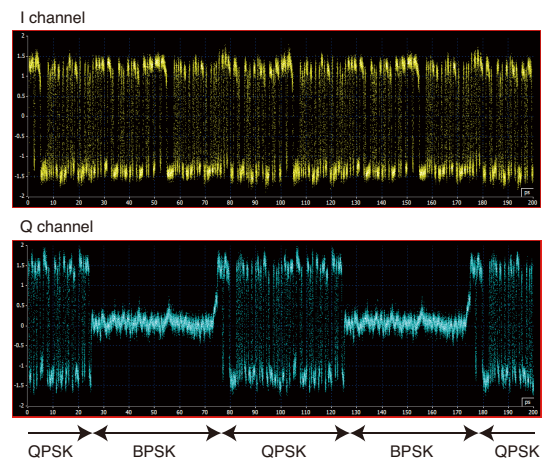


Fig. 2. Temporal development of demodulated I- and Q-channel components.

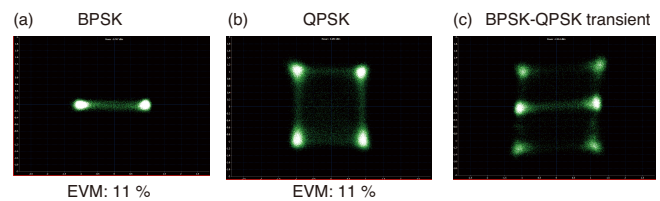


Fig. 3. Observed constellation maps for (a) BPSK, (b) QPSK, and (c) BPSK-QPSK transient signals. The EVMs are also shown.

because the incident binary electrical signal fluctuation is compensated for by the transfer function behavior to form the optical signals. The optimization of the constellation mapping obtained via control of the optical intensity and phase components can generate an optical analogue signal using only the incident binary electrical signals. In other words, the optical IQ modulator operated for QPSK modulation is only used as the 2-bit optical DAC.

The QPSK signal generated by the optical IQ modulator consists of two individual BPSK components with a relative phase of $\pi/2$. If the other BPSK component is turned off, only the optical BPSK signal would be provided by the IQ modulator; this implies the adaptive modulation of BPSK and QPSK signals. For a demonstration of this proof-of-concept, an experimental setup was configured, as shown in Fig. 1(b). A light source was used as a semiconductor laser diode (LD), operated at 1550.116 nm with a line width of less than 100 kHz. A continuous-wave (CW) optical signal was inputted into the optical IQ modulator. The modulator was connected to a two-channel arbitrary waveform generator (AWG) at a sampling speed of 10 GSa/s/ch through optical modulator drivers. The modulated signal was detected and analyzed by an optical modulation analyzer (EXFO, PSO-200). The electrical signal patterns were based on a pseudo-random bit stream (PRBS) with a length of 2^7-1 and $2^{11}-1$. To verify the adaptive modulation, a PRBS signal, whose amplitude were 1 for high a level and -1 for a low level, following a zero signal with the same length as the PRBS was launched to the

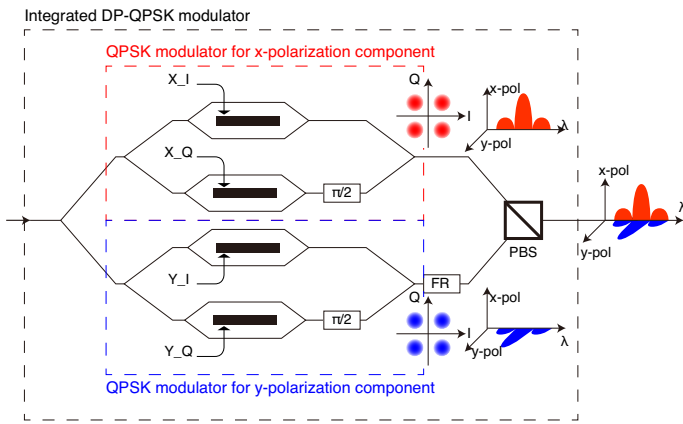


Fig. 4. Schematic of DP-QPSK modulator.

I component of the modulator. For the Q component, a normal PRBS signal was launched. The observed temporal evolution of the I- and Q-channel component of the demodulated optical signals is shown in Fig. 2 for the PRBS-7. Clear switchover behavior between the BPSK and QPSK signals was observed within one bit. This could have been caused by the sampling rate of the AWG. An error vector magnitude (EVM), which corresponds to the Q factor of the optical signal, was estimated to be about 11% for the BPSK and QPSK signals, using constellation maps, as shown in Fig. 3. The temporal evolution of the change in constellation between the BPSK and QPSK signals is also shown in Fig. 3 (c). The superimposition of the QPSK constellation on the BPSK constellation can be clearly observed. The BPSK and QPSK adaptive modulation using the optical IQ modulator was thus successfully demonstrated. It should be noted that the incident electrical signal launched into the I component was some type of a duo-binary signal, and not a simple binary signal. The reason for this is the avoidance of the transient effect of the modulator driver, which was an AC-coupled piece of equipment. For the realization of “real” binary input adaptive modulation, the modulator driver or the electrical signal generator should be equipped with a quick power on/off feature.

B. DP-QPSK Modulator for 16-QAM Generation

An increase in the number of the nested MZIs can realize an increase in the resolution of the optical DAC. A quad-parallel MZI modulator structure for a 4-bit optical DAC, which is a modulator for 16-QAM from four binary electrical signals, has been reported [13]. This optical DAC is based on the coherent synthesis of the independent optical binary signals. Recently, an integrated DP-QPSK modulator was developed for 100GbE, and it consists of two independent QPSK modulators in main MZIs, with a Faraday rotator for polarization rotation in the odd arm. A polarization beam combiner (PBC) was set at the output ports of the two QPSK modulators for polarization division multiplexing (Fig. 4). A coherent synthesis of two polarization QPSK components can also form 16-QAM signals with a polarizer set at an output of the modulator [14]. Because modulator bias voltages could be optimized by a conventional

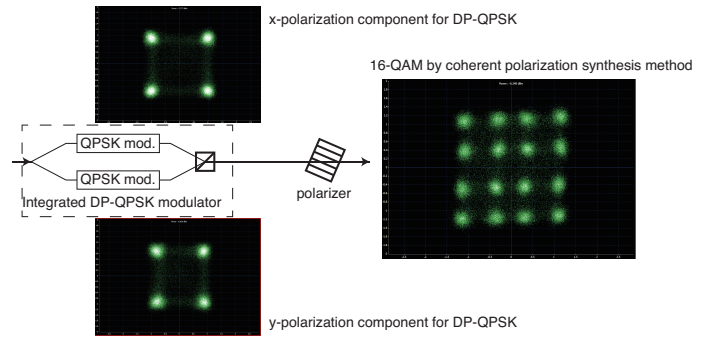


Fig. 5. 16-QAM generation using coherent polarization synthesis method with DP-QPSK modulator. Observed constellation maps for two QPSKs and obtained 16-QAM are also shown.

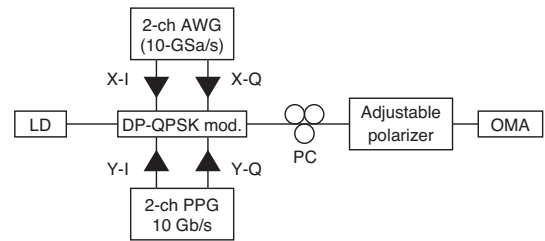


Fig. 6. Experimental setup for QPSK-16QAM adaptive modulation.

QPSK bias controller in each polarization component, optimization of an angle of the polarizer easily provides a 16-QAM signal. The constellations of the DP-QPSK signal and the generated 16-QAM signal with a setup are shown in Fig. 5. Clear symbol separation is observed, with an EVM of around 12%.

A DP-QPSK modulator with an external polarizer would provide adaptive modulation between the QPSK and 16-QAM. The experimental setup, which is shown in Fig. 6, is similar to the BPSK-QPSK adaptive modulation described above. A two-channel pulse pattern generator and a two-channel AWG were connected to the DP-QPSK modulator through the modulator drivers because that modulator had four-channel input for the x-polarization and y-polarization components. The input stream was comprised of a PRBS-11. The polarization of the modulated signal was optimized by a polarization controller, and then, a polarizer formed the 16-QAM with an angle of 130° from the x-axis.

For evaluation of the adaptive modulation, the input pattern for the y-polarization component was set as the PRBS-11 following a zero signal with the same length as the PRBS-11. The modulation format was switched every 204.7 ns between the QPSK and the 16 QAM, which corresponded to the length of the PRBS-11 with 10-Gbaud operation, because the PPG generated the PRBS-11 continuously. The observed temporal evolution of the magnitude and phase components of the demodulated optical signal is shown in Fig. 7. Four-level phase modulation without magnitude fluctuation could be provided by the QPSK signal reception. On the other hand, 16-QAM should provide 4-level amplitude and phase

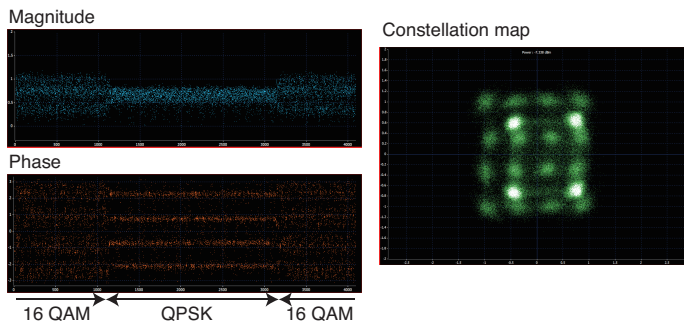


Fig. 7. Temporal evolution of magnitude and phase of received signal between QPSK and 16-QAM adaptive modulation. Constellation map of these transition is also shown.

modulation simultaneously. However, symbol separation could not be observed in the figure. This might be because demodulation could not be completely performed owing to an IQ imbalance caused by a bias voltage drift effect. In general, the bias voltages of the modulator drifted when the amplitude of the launched electrical signal changed considerably. A constellation map that was observed between the QPSK and 16-QAM transition is also shown in Fig. 7, and this behavior seems to have superimposed the QPSK constellation on the 16-QAM constellation. Therefore, it can be considered that adaptive modulation and quick switching between QPSK and 16-QAM was demonstrated with the DP-QPSK modulator. As it is considered with the BPSK-QPSK adaptive modulation by a single QPSK modulator, the DP-QPSK modulator will be applicable to BPSK-QPSK-16-QAM adaptive modulation under high-symbol-rate operation.

III. RADIO-OVER-FIBER SIGNAL GENERATION

High-speed radio communication is also an attractive candidate for high capacity transmission links. RoF technology, which comprises digital and analogue modulation techniques, can provide optically synthesized radio signals with a high symbol rate greater than 10 Gbaud in a millimeter-wave frequency region, and high capacity transmission greater than 50 Gb/s has also been demonstrated [15]–[17]. Generally, a RoF signal consists of an optical local oscillator (LO) component and a baseband component, in which the frequency separation corresponds to the center frequency of the radio signal. Thus, the optical modulators should be set between an optical splitter and a combiner, that is, like an optical MZI configured by optical fibers. However, the path length of each arm in the interferometer can fluctuate owing to the thermal fluctuation of the optical fiber length. This indicates that the phase component of the generated RoF signal could also fluctuate. Therefore, a monolithically integrated MZI is strongly needed with the modulator to produce stable RoF signal generation. A phase-stabilized RoF signal can be provided by an integrated DP-QPSK modulator because this modulator, as described above, comprises two IQ modulators.

Figure 8 shows an example of RoF signal generation using the integrated DP-QPSK modulator. One nested-IQ-modulator

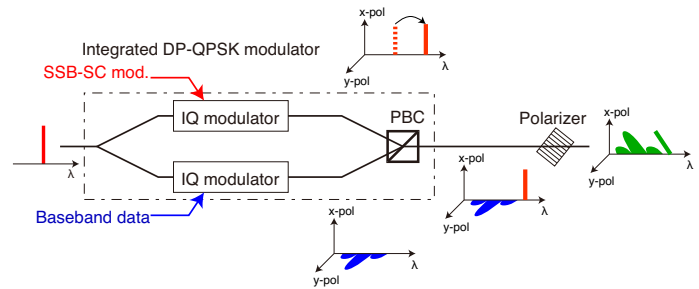


Fig. 8. Schematic diagram of RoF signal generation using integrated DP-QPSK modulator.

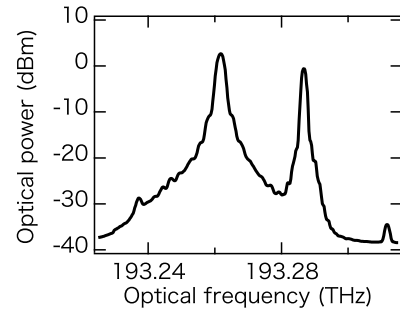


Fig. 9. Optical spectrum of 25-GHz RoF signal observed at the input port of a photomixer.

serves to provide a single-sideband suppressed carrier (SSB-SC) signal [18]. The SSB-SC, which is used as an optical frequency shifter, is realized by two sinusoidal signals with a relative phase of 90° launched into the I and Q ports of the modulator and the main MZI bias of the $\pi/2$ transfer point. When the baseband signal is launched into the other IQ modulator, the RoF signal is formed through the polarizer by means of a technique similar to the one mentioned above. The optimization of the polarization angle can provide adjustment of the power imbalance between the two components.

25-GHz-separated 5-Gb/s QPSK RoF signal generation is shown in Fig. 9 [19]. The baseband component at an optical frequency of around 193.26 THz and a frequency-shifted component from the baseband of 25 GHz at a frequency of around 193.29 THz, which corresponds to the SSB-SC modulation component, can be clearly observed with no significant spurious component. The side-mode suppression ratio of the SSB-SC was about 25 dB. This is caused by the extinction ratio of the nested QPSK modulator of the DP-QPSK modulator.

The RoF signal was directly converted to a radio signal using a 50-GHz-bandwidth photodiode. The generated 25-GHz-band radio signal was acquired by a real-time oscilloscope, whose bandwidth and sampling rate were 30 GHz and 80 GSa/s, respectively, for analysis of the signal quality. The radio power spectrum that was calculated using a fast Fourier transform method from the time evolution signal obtained by the oscilloscope is shown in Fig. 10(a). A 25-GHz-band signal with many spurious components was observed. These

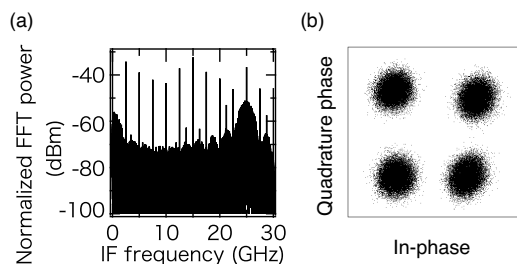


Fig. 10. (a) Observed FFT spectrum of received IF signals and (b) its constellation map.

spurious components could have been caused by leakage of the clock signal because the separation between the spurious components is estimated at about 2.5 GHz, in spite of the fact that there are no spurious components in the optical spectrum in Fig. 9. Thus, the effect of the spurious component is not significant in the RoF signal generation. The observed constellation map of the 2.5-Gbaud QPSK signal is also shown in Fig. 10(b). Clear symbol separation can be seen, with some amplitude and IQ imbalances. These issues could be caused by the amplitude imbalance of the electrical signals launched to the nested QPSK modulator and by the bias voltage misalignment, and therefore, these would be resolved by the optimization. Therefore, the integrated DP-QPSK modulator will be also useful for analogue applications.

IV. CONCLUSION

An integrated optical modulator such as the optical IQ modulator and the DP-QPSK modulator for 100GbE is applicable not only to adaptive digital modulation with a high symbol rate and high switching speed, but also to analogue applications such as RoF signal generation. This signal generation technique is based on the scheme of the optical DAC, and thus, a high level of parallelism of the modulator can realize a high resolution and complicated signal generation. These optical modulators developed for optical fiber communication might also be applicable to free-space optical communication for GND-LEO, GND-GEO, and GND-deep-space satellites.

ACKNOWLEDGMENTS

The authors would like to thank Mr. Takaya Murakami of Marubun Corporation and Mr. Chee Wee Lim, Mr. Ray Chong, and Mr. Jean-Sebastien Tasse of EXFO for allowing them to use their latest optical modulation analyzer. The authors would also like to thank Mr. Yoichi Hosokawa, Mr. Kaoru Higuma, and Dr. Junichiro Ichikawa of Sumitomo Osaka Cement Co. Ltd. for their fruitful discussions and for allowing them to use their DP-QPSK modulator.

REFERENCES

- [1] The NTT Group's response to the Great East Japan Earthquake; http://www.ntt.co.jp/csr_e/2011report/
- [2] JAXA press release, "KIZUNA's Support Activities for Disaster-stricken Areas after Tohoku Region Pacific Ocean Coastal Earthquake," http://www.jaxa.jp/press/2011/03/20110320_kizuna_e.html
- [3] S. Arnon, "Power Versus Stabilization for Laser Satellite Communication," *Applied Optics*, vol. 38, iss. 15, pp. 3229–3233 (1999).

- [4] M. Toyoshima, Y. Takayama, T. Takahashi, K. Suzuki, S. Kimura, K. Takizawa, T. Kuri, W. Klaus, M. Toyoda, H. Kunimori, T. Jono, K. Arai, "Ground-to-satellite laser communication experiments," *IEEE Aerospace and Electronic Systems Mag.*, vol. 23, Iss. 8, pp. 10–18 (2008).
- [5] V. W. S. Chan, "Space coherent optical communication systems—An introduction," *J. Lightw. Tech.*, vol. 5, iss. 4, pp. 633–637 (1987).
- [6] R. Lange, F. Heine, H. Kämpfner, and R. Meyer, "High Data Rate Optical Inter-Satellite Links," in *35th Euro. Conf. Opt. Commun.*, Vienna, Austria, Symp.10.5.1 (2009).
- [7] D. O. Caplan, H. Rao, J. P. Wang, D. M. Boroson, J. J. Carney, A. S. Fletcher, S. A. Hamilton, R. Kochhar, R. J. Magliocco, R. Murphy, M. Norvig, B. S. Robinson, R. T. Schulein, and N. W. Spellmeyer, "Ultra-Wide-Range Multi-Rate DPSK Laser Communications," in *Conference on Lasers and Electro-Optics*, San Jose, USA, paper CPDA8 (2010).
- [8] J. Anderson, "Optical transceivers for 100 gigabit Ethernet and its transport [100 gigabit ethernet transport]," *IEEE Commun. Mag.*, vol. 48, iss. 3, pp. S35–S40 (2010).
- [9] A. Kanno, T. Sakamoto, A. Chiba, T. Kawanishi, M. Sudo, K. Higuma, J. Ichikawa, "95-Gb/s NRZ-DPSK Modulation with Full-ETDM Technique," in *Euro. Conf. Opt. Commun.*, Turin, Italy, Mo.2.F.5 (2010).
- [10] H. Yamazaki, T. Yamada, T. Goh, Y. Sakamaki, A. Kaneko, "64QAM Modulator With a Hybrid Configuration of Silica PLCs and LiNbO₃ Phase Modulators," *IEEE Photon. Tech. Lett.*, vol. 22, iss. 5, pp. 344–346 (2010).
- [11] A. Kanno, T. Sakamoto, A. Chiba, T. Kawanishi, M. Sudo, K. Higuma, J. Ichikawa, "90 Gbaud NRZ-DP-QPSK Modulation with Full-ETDM Technique Using High-Speed Optical IQ Modulator," *IEICE Trans. Electron.*, vol. E94-C, no. 7, pp.1179–1186 (2011).
- [12] G. Raybon, P. J. Winzer, A. A. Adamiecki, A. H. Gnauck, A. Konczykowska, F. Jorge, J.-Y. Dupuy, L. L. Buhl, C. R. Doerr, R. Delbue, P. J. Pupalakis, "All-ETDM 80Gbaud (160Gb/s) QPSK Generation and Coherent Detection," *IEEE Photon. Tech. Lett.*, vol. 23, iss. 22, pp. 1667–1669 (2011).
- [13] T. Sakamoto, A. Chiba, T. Kawanishi, "50 Gb/s 16 QAM by a quad-parallel Mach-Zehnder modulator," in *Euro. Conf. Opt. Commun.*, Berlin, Germany, paper PD2.8 (2007).
- [14] I. Morohashi, M. Sudo, T. Sakamoto, A. Kanno, A. Chiba, J. Ichikawa, T. Kawanishi, I. Hosako, "16 Quadrature Amplitude Modulation Using Polarization-Multiplexing QPSK Modulator," *IEICE Trans. Commun.* vol. E94-B, no. 7, pp. 1809–1814 (2011).
- [15] A. Kanno, K. Inagaki, I. Morohashi, T. Sakamoto, T. Kuri, I. Hosako, T. Kawanishi, Y. Yoshida, K. Kitayama, "20-Gb/s QPSK W-band (75–110 GHz) wireless link in free space using radio-over-fiber technique," *IEICE Electron. Express*, vol. 8, no. 11, pp. 612–617 (2011).
- [16] X. Pang, A. Caballero, A. Dogadaev, V. Arlunno, R. Borkowski, J. S. Pedersen, L. Deng, F. Karinou, F. Roubeau, D. Zibar, X. Yu, and I. T. Monroy, "100 Gbit/s hybrid optical fiber-wireless link in the W-band (75–110 GHz)," *Optics Express*, vol. 19, iss. 25, pp. 24994–24949 (2011).
- [17] A. Kanno, K. Inagaki, I. Morohashi, T. Sakamoto, T. Kuri, I. Hosako, T. Kawanishi, Y. Yoshida, K. Kitayama, "40 Gb/s W-band (75–110 GHz) 16-QAM radio-over-fiber signal generation and its wireless transmission," *Opt. Express*, vol. 19, no. 26, pp. B56–B60 (2011).
- [18] T. Kawanishi, T. Sakamoto, and M. Izutsu, "High-Speed Control of Lightwave Amplitude, Phase, and Frequency by Use of Electrooptic Effect," *J. Sel. Top. Quantum Electron.*, vol. 13, pp. 79–91 (2007).
- [19] T. Fujita, R. Yamanaka, A. Kanno, T. Kawanishi, H. Sotobayashi, "25-GHz-Band RoF Signal Generation Using Dual-Polarization QPSK Modulator," in *Asia-Pacific Microw. Photon. Conf.*, Kyoto, Japan, paper WC-5 (2012).